BURIED MINE DETECTION BY POLARIMETRIC RADAR INTERFEROMETRY

L. Sagués[1] , Juan M. López-Sánchez[2], J. Fortuny[3]
X. Fàbregas[1], A. Broquetas[4] , A. J. Sieber[3]

[1]Dpt. Teoria del Senyal i Comunicacions
Universitat Politècnica de Catalunya (UPC)
Campus Nord UPC, c/ Jordi Girona, 1-3, 08034 Barcelona, Spain
[2]Depto. Física, Ing. Sistemas y Teoría de la Señal
Universidad de Alicante
P.O. Box 99, E-03080 Alicante, Spain
[3]Space Applications Institute, Joint Research Centre
SAI, TP.272, 21020 Ispra, Italy
[4]Institute of Geomatics
Parc de Montjuïc, E-08038, Barcelona, Spain

INTRODUCTION

Nowadays, subsurface detection of objects is a challenge for the scientific community since it would give a solution to actual humanitarian and civil problems, such as de-mining. A large number of remote sensing techniques has been considered as candidates for this task at a safe stand-off distance. To date, several promising results have shown that ultra-wide band SAR sensors can detect most metallic mines. However, buried plastic mines are nearly invisible to the radar and can not be easily detected due to the fact that the dielectric contrast between the target and the soil is insignificant[1]. Moreover, the weak signal returned from the mine is normally hidden in strong surface clutter, making its detection more complicated.

In this context, Polarimetric SAR Interferometry is a new technique that can be applied to enhance the discrimination between targets and clutter. It is well known that conventional SAR interferometry uses relative phase information from two radar images acquired from different viewing angles in order to estimate the height of ground scatterers. On the other hand, radar polarimetry allows us to extract target information from the measurements of the state of polarisation of the scattered wave, making possible to decompose the target into different scattering behaviours. Therefore, by combining both polarimetry and interferometry it would be possible to get the height of different scattering mechanisms that can be present in the same resolution cell, even if one scattering process is much weaker than the other[2]. The objective of the polarimetric and interferometric

Ultra-Wideband, Short-Pulse Electromagnetics 5
Edited by P. D. Smith and S. R. Cloude, Kluwer Academic/Plenum Publishers, 2002

approach presented in this paper is to separate the phase centre corresponding to the mine from that related to the clutter and estimate their relative height.

Several multifrequency experiments have been carried out in the anechoic chamber of the European Microwave Signature Laboratory (EMSL) at JRC Ispra[4] to test the application of this new technique for buried mine detection. Fully coherent polarimetric data were collected at L, S and C band. The target was formed by four plastic mines and a metallic cylinder, that were buried below a thick layer of gravel. The obtained results will be shown and discussed in this paper.

MINE DETECTION USING POLARIMETRIC SAR INTERFEROMETRY

SAR Interferometry

The geometry of an interferometric imaging system is illustrated in Fig. 1. The interferogram is formed by cross-multiplying two SAR images obtained from slightly different viewing angles. The antennas are located at two different positions A_1 and A_2, illuminating the same patch on the surface at two incidence angles θ_1 and θ_2, respectively. The distance between the two antenna positions is known as the baseline B, whereas the distances from each antenna to the centre of the resolution cell are r_1 and r_2.

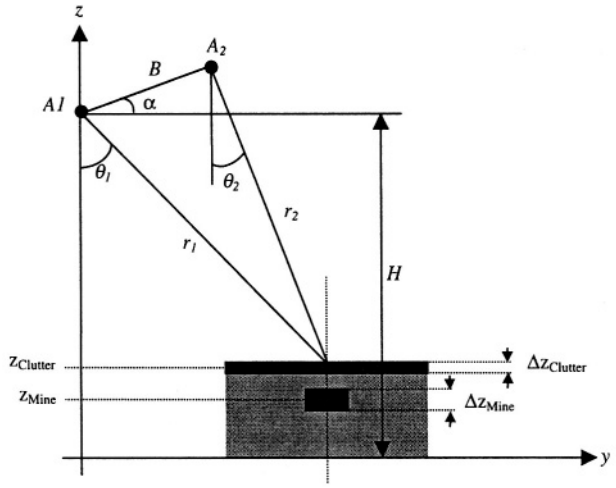

Figure 1. Interferometric SAR system operating in a buried mine scenario

The interferogram is generated by multiplying an image by the complex conjugate of the other. Thus, the phase of the interferogram corresponds to the phase difference between both SAR images:

$$\phi_{\text{int}} = angle\{s_1 s_2^*\} = \phi_1 - \phi_2 = \frac{4\pi}{\lambda}(r_2 - r_1) = \frac{4\pi}{\lambda}\Delta r \tag{1}$$

Since the phase of each SAR image is related to the distance between the antennas and the ground, we can derive a relationship between this travel path difference and the local height of each ground scatterer:

$$\sin(\alpha-\theta)=\frac{(r+\Delta r)^2-r^2-B^2}{2rB}$$
$$h=H+r\cos\theta \tag{2}$$

whereby we can generate an elevation map of the scene under observation. Thus, an additional height dimension is introduced in the reflectivity images. The quality of the generated elevation map depends on the quality of the interferometric phase. The parameter used to evaluate the phase quality is the so-called interferometric coherence, which can be interpreted as a useful tool for measuring the resemblance (correlation) between the two SAR images:

$$\gamma=\frac{\langle s_1 s_2^* \rangle}{\sqrt{\langle |s_1|^2 \rangle \langle |s_2|^2 \rangle}} \tag{3}$$

If the coherence equals to zero, it would mean the scene is completely uncorrelated and then the interferogram is noisy and not related to the topography. At the other extreme, a coherence close to one corresponds to a noise-free interferogram from which a high quality elevation map can be generated.

In a real buried mine scenario, as shown in Figure 1, the mine is confounded into the clutter and there exists an uncertainty in determining the interferometric phase due to the existence of different scattering centres inside the resolution cell. As a consequence of this, the coherence degrades and it is not possible to extract the height of the mine accurately. Therefore, it would be useful to separate the scattering mechanism related to the mine from that corresponding to the clutter surface in order to get their height independently. If the choice of these scattering mechanisms is based on selecting those polarisation states that maximise the interferometric coherence, then the interferometric phase associated with them presents a better quality and the accuracy of their height estimation is higher. Two different polarimetric coherence optimisation algorithms can be applied to extract this height information. The original optimisation algorithm, presented by Cloude[2], formulates the exact formal solution of the coherence maximisation problem, leading to two complex 3x3 eigenvalue problems that share the same eigenvalues. The three derived eigenvalues are related to pairs of eigenvectors that can be interpreted as the optimum scattering mechanisms. The second method, called Polarisation Subspace Method (PSM) is described in next section. This alternative approach is based on finding the local maxima of those copolar or crosspolar coherence function that have been calculated from the measurements of all polarisation states of the scattered wave[3].

Polarisation Subspace Method

If fully coherent polarimetric data are collected, the information associated with each pixel of the SAR image is then defined by the following scattering vector:

$$\vec{k}=\left[S_{hh},\sqrt{2}S_{hv},S_{vv}\right]^T \tag{4}$$

where S_{mn} is the complex scattering coefficient for n transmitted and m received polarisation expressed in the orthogonal (H,V) basis. In case of interferometric

measurements, the polarimetric information will be contained in two different scattering vectors, k^1 and k^2, for image 1 and image 2 respectively, leading to the following hermitian matrices:

$$[C^{ij}] = \left\langle \vec{k}^{i}\, \vec{k}^{j\,*T} \right\rangle = \begin{bmatrix} \left\langle S^i_{hh} S^{j\,*}_{hh} \right\rangle & \sqrt{2}\left\langle S^i_{hh} S^{j\,*}_{hv} \right\rangle & \left\langle S^i_{hh} S^{j\,*}_{vv} \right\rangle \\ \sqrt{2}\left\langle S^i_{hv} S^{j\,*}_{hh} \right\rangle & 2\left\langle S^i_{hv} S^{j\,*}_{hv} \right\rangle & \sqrt{2}\left\langle S^i_{hv} S^{j\,*}_{vv} \right\rangle \\ \left\langle S^i_{vv} S^{j\,*}_{hh} \right\rangle & \sqrt{2}\left\langle S^i_{vv} S^{j\,*}_{hv} \right\rangle & \left\langle S^i_{vv} S^{j\,*}_{vv} \right\rangle \end{bmatrix} \tag{5}$$

where *i=1,2* and *j=1,2* refers to each SAR image used to form the interferogram. Thus, $[C^{11}]$ and $[C^{22}]$ are the two covariance matrices associated with the separate images, whereas $[C^{12}]$ is a 3 x 3 complex matrix which contains the interferometric information between polarimetric channels.

Otherwise, instead of using a linear polarisation basis to describe the vector fields, one can use any other orthogonal elliptic basis. The coordinates transformation of a scattering vector from the linear basis (h,v) to another orthonormal elliptic basis (x,y) can be accomplished by applying a unitary matrix transformation $[U_3]$ to the polarisation vector[3]:

$$\vec{k}' = \left[S_{xx}, \sqrt{2}S_{xy}, S_{yy}\right] = [U_3]_{(\phi,\tau)}\, \vec{k} \tag{6}$$

where τ and ϕ are the ellipticity and inclination angles that define any polarisation state. Physically, this transformation can be interpreted as a change of the selected scattering mechanisms in both images. After applying this polarisation basis change, we can express the covariance matrices defined in (5) in any different polarisation state (ϕ,τ):

$$[C^{ij}]_{(\phi,\tau)} = \left\langle [U_3]\vec{k}^{\,i}\vec{k}^{\,j\,*T}\,[U_3]^{*T} \right\rangle = [U_3][C^{ij}][U_3]^{*T} \tag{7}$$

The application of these polarimetric basis transformations enables the formation of interferograms between all possible elliptical polarisation states and polarimetric combinations between both SAR images. In this way, the interferometric coherence between all polarimetric combinations will be given by:

$$\left|[\Gamma']_{(\phi,\tau)}\right| = \left[\frac{\left|c^{12'}{}_{mn}\right|}{\sqrt{c^{11'}{}_{mn} \cdot c^{22'}{}_{mn}}} \right]_{\substack{1\le m\le 3 \\ 1\le n\le 3}} = \begin{bmatrix} \gamma_{xx-xx} & \gamma_{xx-xy} & \gamma_{xx-yy} \\ \gamma_{xy-xx} & \gamma_{xy-xy} & \gamma_{xy-yy} \\ \gamma_{yy-xx} & \gamma_{yy-xy} & \gamma_{yy-yy} \end{bmatrix} \tag{8}$$

being $c^{ij}{}_{mn}$ the elements of the covariance matrices defined in (7). The optimum interferogram will be generated by selecting that combination of polarisation states (ϕ,τ) which maximise the interferometric coherence Γ'. Once the interferometric phase is calculated, it can be converted to absolute height by using the conventional interferometric phase-to-height equations described in (2):

$$\left|[H]_{(\phi,\tau)}\right| = = \begin{bmatrix} h_{xx-xx} & h_{xx-xy} & h_{xx-yy} \\ h_{xy-xx} & h_{xy-xy} & h_{xy-yy} \\ h_{yy-xx} & h_{yy-xy} & h_{yy-yy} \end{bmatrix} \tag{9}$$

We can further simplify this approach by using some *a priori* knowledge about the values in $\Gamma'(\phi,\tau)$. The first assumption is that, in cases where there is no temporal

decorrelation and the baseline is short, the highest coherence will be given by the same polarisation state in both images, and therefore the elements of the diagonal of the matrix Γ' will be much higher than the rest. Moreover, the definition of the geometrical angles implies the following transformation symmetry:

$$\gamma_{xx-xx}(\phi,\tau)=\gamma_{yy-yy}(\phi+\pi/2,-\tau) \tag{10}$$

and, consequently, if the assumption is valid, we must calculate only the first and the second elements of the diagonal of Γ' and select the maximum one:

$$\gamma(\phi_{opt},\tau_{opt})=max\{\gamma_{xx-xx}(\phi,\tau),\gamma_{xy-xy}(\phi,\tau)\} \tag{11}$$

This optimisation method is called Polarisation Subspace Method (PSM) because we are only considering the copolar and crosspolar elements, and the same basis polarisation transformation is applied in both images.

This method can not only be used for getting the optimum scattering mechanism that maximise the coherence but also for deriving the height structure of the target. By graphically representing the copolar and crosspolar coherence functions, it is possible to derive the existence of independent scattering mechanisms inside the same resolution cell. In case of a single dominant scattering behaviour, both coherence functions generally present only one absolute maximum. However, in those cases where the target presents a clear multilayer vertical structure, as shown in Figure 1, it is possible to identify various local coherence maxima. These optimum polarisation states will be related to different independent scattering mechanisms that lead to the locally best height estimation. In case of buried mine detection, it is expected to find two coherence maxima, each of them related to a different scattering mechanism located at a different height: the mine and the surface clutter (or air-ground interface). After generating the two interferograms corresponding to these optimum polarisation states, we can extract the height difference between them. The resulting height difference map will exhibit some peaks at those positions where the mines are buried whereas it will remain close to zero at those zones of the image where only a single surface scattering process can be found.

EXPERIMENTAL RESULTS

Several multifrequency experiments were carried out in the anechoic chamber of the European Microwave Signature Laboratory (EMSL) at JRC Ispra, Italy. The experimental setup is shown at Fig. 2. Four plastic mines and a metallic cylinder were buried below a thick layer of gravel. Mine 1 and mine 4 were buried at 20 cm depth under the surface, whereas the other two mines were buried at 10 cm depth. The separation between mines was 80 cm and their size was different: the diameter of mines 1 and 2 was 20 cm, whereas the diameter of mines 3 and 4 was 25 cm. The cylinder was in the middle of the four mines and it was buried at 10 cm depth. Fully coherent polarimetric data were collected for different baselines, covering the frequency range from 2 GHz to 6 GHz.

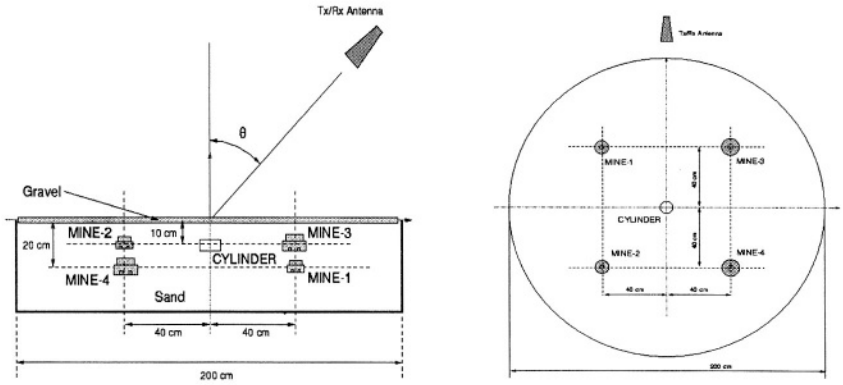

Figure 2. Experimental setup: side (left) and top (right) view

Fig. 3 shows the reconstructed SAR images using HH and VV polarisation for a frequency range between 2 GHz and 3 GHz. The resolution cell was about 20 cm in both dimensions. As can be seen, the metallic cylinder is detected and located 15 cm far from the centre of the scene because the image was focused at the gravel reference level. However, the four plastic mines can not be distinguished using the amplitude reflectivity image because the strong surface clutter masks the mine backscattering response.

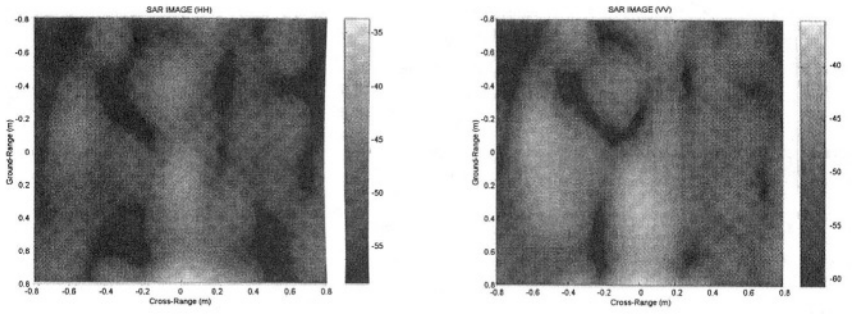

Figure 3. HH (left) and VV (right) SAR amplitude images

After applying the Polarisation Subspace Method, we can notice that the coherence copolar coherence function $\gamma_{xx\text{-}xx}\ (\phi,\tau)$ exhibits two local maxima when the method is applied at those zones of the scene where a mine was buried. As an example, Fig. 4 depicts the obtained coherence function and the resulting absolute height $h_{xx\text{-}xx}$ for all (ϕ,τ) polarisation states when calculating them inside a 60 x 60 cm window centred at mine 3 location. The two local maxima appear at $(\phi_1 = 10°,\ \tau_1 = 42°)$ and $(\phi_2 = 44°,\ \tau_2 = -22°)$. The absolute height associated with the first state of polarisation is -0.7 cm, which is very close to the surface reference height, whereas the height derived from the second one is 8.54 cm. Therefore, we can state that the first one corresponds to the surface scattering mechanism while the second one is related to the buried mine. The height difference between both polarisation states results 9.24 cm, which is very close to the actual depth of mine 3 (10

cm). It is important to note that this result has been obtained by applying a multi-look procedure (spatially averaging of N = 9 resolution cells) in order to reduce the height standard deviation.

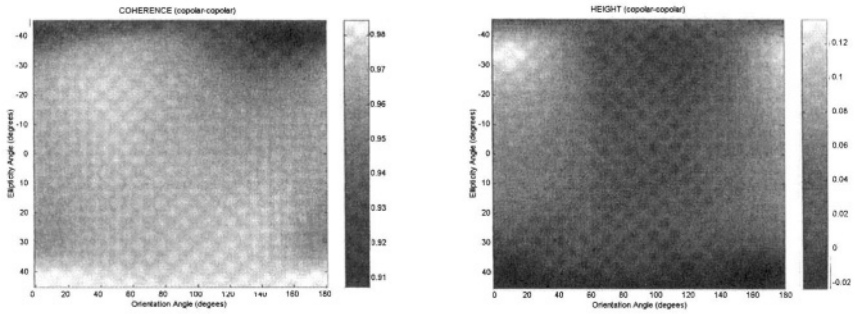

Figure 4. Coherence (left) and elevation maps (right) for all polarisation states

This procedure can be applied to the entire surface by sliding the averaging window on the resulting complex interferograms. However, it is not possible to consider a high number of spatial looks during the averaging process because it implies a loss of spatial resolution. Fig. 5 shows the elevation map obtained by calculating the height difference between those polarisation states that maximise the copolar coherence function, for a frequency range from 2 up to 3 GHz. As can be seen, the resulting height difference increases at those zones where the mines were buried, but it remains close to zero for the rest. Therefore, the four buried mines can be clearly detected. Nevertheless, we can note that the metallic cylinder is not detected at this low frequency band. The reason is that the ground attenuation is low and the resulting cylinder scattering amplitude is too high compared to the surface one. Consequently, the copolar function, calculated at the cylinder zone, exhibits only a single maximum that corresponds to the cylinder height.

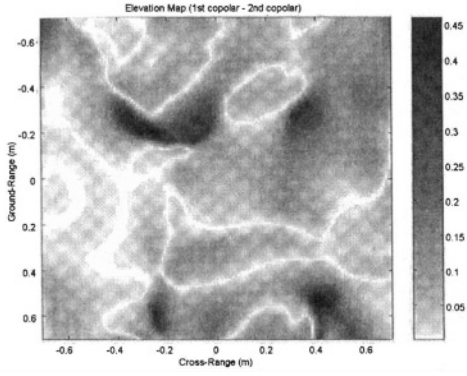

Figure 5. Height difference between the two optimum copolar polarisations at 2 - 3 GHz

However, if we apply the same method at higher frequencies (4 – 5 GHz), an additional second maximum, which corresponds to the surface response, appears in the copolar coherence function. Hence, after calculating the height difference between both optimum states of polarisation, we obtain the result shown in Fig. 6. Note that in this case the cylinder is well detected whereas the mines can not be distinguished.

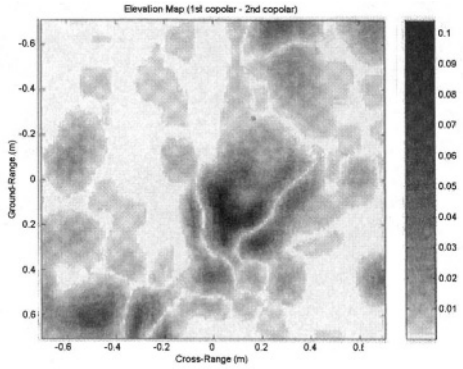

Figure 6. Height difference between two optimum copolar polarisation states at 4 - 5 GHz

Thus, we can conclude that the polarimetric method here presented has a strong dependency on the operating frequency. This can be clearly noticed by representing a cut of the obtained height difference along the ground-range axis where mine 3 and mine 4 were buried, for different frequency ranges (see Fig. 7). The obtained height values are higher than expected due to that no multi-look procedure has been applied in order to preserve the spatial resolution and extract the correct position of the mines. Note that both mines are only detected with the lowest frequency band (2 – 3 GHz). At higher frequencies, the ground attenuation weaken the mine signal, and only one optimum polarisation state can be derived from the copolar coherence function.

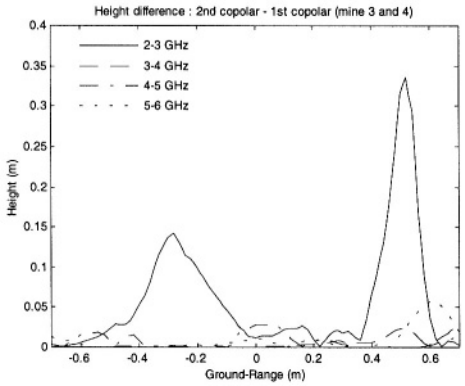

Figure 7. Height difference for x = 0.4 m as a function of the frequency range

CONCLUSIONS

In this paper we have presented a new polarimetric and interferometric approach that can be applied to improve the sub-clutter visibility in de-mining applications. The obtained experimental results have shown that buried plastic mines can not be detected by using only SAR images. However, after applying the method presented here, it is possible to separate the scattering mechanism that is associated with the clutter surface from that corresponding to the mine and estimate their height location. Nevertheless, the success of the proposed method will depend on the geometry of the problem. Indeed, it is necessary the surface clutter to be physically separated from the mine in order to distinguish both scattering mechanisms by optimising the interferometric coherence.

It has also been proved that the probability of detection shows a strong dependency on the frequency range. In case of detecting plastic mines, we have seen that it is convenient to operate at low frequencies in order to reduce the attenuation caused by ground propagation. On the other hand, multi-look averaging techniques must be applied in order to reduce the false alarm rate and improve the height estimation accuracy, at the expense of loosing spatial resolution.

Acknowledgments

The authors wish to thank the CICYT (Spanish Commission for Science and Technology) ref TIC99-1050-C03-01 for their financial support. This work has been carried out in the frame of the European Commission TMR Network on radar polarimetry.

REFERENCES

1. L. Carin, N. Geng, M. McClure, J. Sichina, L. Nguyen, Ultra-wide band synthetic aperture radar for mine-field detection, *IEEE Antennas and Propagation Magazine,* 18:33(1999).
2. S.R. Cloude, K.P. Papathanassiou, "Polarimetric SAR Interferometry", *IEEE Trans, on Geoscience and Remote Sensing,* 1551:1565(1998).
3. L. Sagués, J.M. López-Sánchez, J. Fortuny, X. Fàbregas, A. Broquetas, A.J. Sieber, "Indoor Experiments on Polarimetric SAR Interferometry", *IEEE Trans. on Geoscience and Remote Sensing,* 671:684 (2000).
4. A.J. Sieber, "The European Microwave Signature Laboratory", *EARSel Advances in Remote Sensing,* 195:201 (1993).